Published in final edited form as:
Int J Hyperthermia. 2013 June ; 29(4): 346–357. doi:10.3109/02656736.2013.790092.

Simulation techniques in hyperthermia treatment planning

MM Paulides[1], **PR Stauffer**[2], **E Neufeld**[3], **P Maccarini**[2], **A Kyriakou**[3], **RAM Canters**[1], **C Diederich**[4], **JF Bakker**[1], and **GC Van Rhoon**[1]

[1]Erasmus MC Cancer Center, Rotterdam, The Netherlands [2]Duke University Medical Center, Durham NC, USA [3]IT'IS, Foundation for Research on Information Technologies in Society, Zurich, Switzerland [4]UCSF, San Francisco CA, USA

Abstract

Clinical trials have shown that hyperthermia (HT), i.e. an increase of tissue temperature to 39-44°C, significantly enhance radiotherapy and chemotherapy effectiveness (1). Driven by the developments in computational techniques and computing power, personalized hyperthermia treatment planning (HTP) has matured and has become a powerful tool for optimizing treatment quality. Electromagnetic, ultrasound, and thermal simulations using realistic clinical setups are now being performed to achieve patient-specific treatment optimization. In addition, extensive studies aimed to properly implement novel HT tools and techniques, and to assess the quality of HT, are becoming more common. In this paper, we review the simulation tools and techniques developed for clinical hyperthermia, and evaluate their current status on the path from “model” to “clinic”. In addition, we illustrate the major techniques employed for validation and optimization. HTP has become an essential tool for improvement, control, and assessment of HT treatment quality. As such, it plays a pivotal role in the quest to establish HT as an efficacious addition to multi-modality treatment of cancer.

Keywords

SAR; Thermal; Electromagnetic; Ultrasound; Pennes Bioheat Equation

Introduction

Hyperthermia treatment planning (HTP) is defined as the process that begins with obtaining patient data and establishing, by electromagnetic (EM), ultrasound (US), and/or thermal modeling, a set of treatment parameters that maximize treatment quality. The taskforce report of European society for hyperthermic oncology (ESHO) and committee for concerted action in bio-medical engineering (COMAC BME) of 1992 (2) was the first comprehensive document to summarize all available techniques and measurement data required for HTP and validation. The topical review by Lagendijk (3) extended that work to include thermal techniques, and described the state of the art in HTP in 2000. In the last decade, significant progress has been made on the availability and accuracy of EM and US simulation tools and techniques. In addition, thermal simulations based on the Pennes bioheat equation (PBHE) (4) have been implemented in commercial software packages for clinical planning. The importance of HTP in the current clinical setting is illustrated by the recent decision of ESHO to include HTP in their quality assurance guidelines for deep hyperthermia (5, 6).

Correspondence: m.paulides@erasmusmc.nl, Tel: + 31 10 7041610/Fax: +31 10 7041022.

Declaration of interest: The authors alone are responsible for the content and writing of this paper.

In this paper, we describe a selection of tools and techniques that are being used for planning and guiding hyperthermia (HT) treatments. Specifically, we analyze EM, US, and thermal simulation tools and techniques, with a strong focus on the potential to improve clinical results. In addition, we address methods to perform validation of numerical algorithms. Also, we describe methods to quantify the influences of those uncertainties that cannot be controlled. Finally, we describe how HTP can be used, not only for pre-planning, but also in feedback control strategies and to assess the overall quality of treatment.

Hyperthermia treatment planning

Simulations for HTP can be divided into three distinct tasks:

1. generation of the patient model.
2. calculation of the distribution of power deposited in the tissue.
3. calculation of the resulting temperature distribution in the tissue.

First, the geometry and tissue properties of the involved body region must be carefully identified. Several companies have preprocessed and made available human body models of typical adult male, adult female, and small child anatomies that have geometric, electromagnetic, and thermal properties included. For improved accuracy, patient specific modeling is performed by segmenting tissues using computed tomography (CT) or magnetic resonance (MR) images of the actual subject. Next, the specific absorption rate (SAR), or more generally the power density (PD), distribution, is determined by EM or US modeling approaches. Once the PD pattern is established, the temperature (T) distribution can be predicted based on thermal redistribution of energy within the heated region with consideration of the impact of physiological aspects such as perfusion and core temperature. While SAR modeling has matured, and good accuracy is now possible in some EM applications (7), there are limitations due to imprecise modeling of patient anatomy, tissue interfaces, and tissue properties. In addition, for EM-HTP, there are still difficulties in modeling the behavior of some applicators, e.g. due to the impact of loading conditions and cross-coupling. For US-HTP, full wave modeling of acoustic propagation and the computational requirements remain an issue. Accurate prediction of T distributions with thermal modeling is an even greater challenge. Large deviations in thermal tissue properties and their variation during the course of heating make *in vivo* temperatures difficult to predict. Hence, although the temperature level achieved throughout the tumor is believed to determine treatment quality, optimization of heating in current clinical applications is often performed by optimizing the SAR distribution (8). Figure 1 provides a scheme of the steps required for HTP. In step one, CT or MR imaging data is converted into a 3D representation of the patient by delineating different normal and tumor or target tissue regions. 3D models are obtained by assigning corresponding electrical, ultrasonic, and thermal properties to each 3D tissue structure. Next, a model of the applicator with the required degree of complexity and the patient model are combined and used to compute the PD and thermal distributions. Optimization of these distributions can be performed at the PD or temperature “level”. It is also possible to combine the optimization and thermal simulation steps (9, 10).

3D patient modeling

Patient modeling is an important but challenging part of HTP. Time-efficient and easy-to-use segmentation algorithms for delineation of tissues on CT or MR data are a precondition for the 3D models that are required for clinical application of patient-specific HTP (11). The required detail of the models depends on the desired accuracy, which should be assessed carefully for each application. Typically requirements are far higher than for example in radiotherapy, as more tissues need to be distinguished to correctly capture the important

impact of strong dielectric property and perfusion variations between tissues, e.g. for hot-spot prediction. Investigators have identified substantial dependences of PD and temperature distributions on both the patient models and the temperature algorithm used (3, 12, 13). Wust et al. showed that surface models, i.e. delineated tissue boundaries for each distinct organ or tissue region, each with assigned homogenous dielectric properties, match clinical results better than models that attempt to derive heterogeneous dielectric properties directly from CT data (14, 15). Similar results were obtained from attempts to use to MR-derived heterogeneous tissue models (16, 17). Ever since, surface models have become the standard, especially for EM-HTP. Tissue properties, however, are non-homogeneous and vary between patients. For dielectric properties, variations of 30% or more have been measured in postmortem humans (18, 19), and even greater variations were shown in breast (20, 21) and brain, by means of MR measurements (22). Fortunately, the influence of those uncertainties on the SAR of deep-regional phased-array applicators has been found to be typically less than 10% (23, 24).

Creating surface models of numerous organs from CT and/or MRI data of each patient requires many man-hours and, which hinders clinical acceptance. Therefore, researchers have begun investigating the increase in segmentation speed and reduction in operator time demands offered by atlas-based segmentation techniques (25, 26). This semi-automatic method requires a library of accurately segmented patient models that incorporate all the relevant tissue-shape variations.

Power absorption simulation techniques

Electromagnetic

In the past three decades, many numerical techniques have been applied in the simulation of EM thermal therapy for cancer. Excellent reviews on numerical codes can be found in Hand *et al.* (27) and Deuflhard *et al.* (28) summarized the mathematics required in deep-regional hyperthermia.

In addition to a good patient model, the applicator model is very important for the treatment plan quality. Progress in computation tools now allow generation of more-precise 3D representations of the applicator, e.g., in CAD format, for realistic EM simulations. In addition to physical geometry, the model must numerically reproduce the applicator behavior and its interaction with the tissue, which requires careful discretization and source implementation in the EM model (29). The resolution required for the model depends on the numerical technique and applicator type. Modeling the antenna excitation is also critically important, especially for quantitative SAR prediction (29). In general, an experienced EM designer must make suitable simplifications, and the EM model must be validated first in flat or cylindrical phantoms before proceeding to complex heterogeneous tissue geometries. In addition, applicators should be designed such that they facilitate accurate modeling, e.g., low dependence on load impedance and good control of cross-coupling between antennas.

Achieving maximum benefit from HTP requires a sound translation of the model setup and parameters into the clinic. Translation errors in transferring the applicator settings from the HTP system to the treatment room can seriously reduce the benefit of HTP parameter optimizations. Numerous studies have shown the importance of establishing uncertainties and validating calculated output parameters. Parameters studied for phased arrays are intensity, i.e. amplitude or power, and phase-differences between the antenna drive signals (30-33). Further, variation in the position of the patient relative to the antenna array has been shown to be critically important (34). Also, the posture of the patient during CT or MR image acquisition should match that used for the HT treatment to avoid planning errors. Finally, the shape of the water bolus must be accurately modeled. Uncertainties in water

bolus shape have been shown to be important both in superficial (35, 36) as well as deep-regional hyperthermia (34).

HT treatments are normally limited by hotspots in healthy tissue. For EM HT, these are typically caused by electric (E) field maxima at locations with high dielectric contrast (e.g. bone-muscle interfaces). To minimize these hotspots, several objective functions are utilized to optimize antenna phase and amplitude excitation parameters (37). Other parameters, such as patient positioning, are typically not optimized due to the associated prohibitive effort. Optimization is highly application-specific, and numerous papers have been published on phase/amplitude optimization of array applicators (37-45). For some optimization functions, specialized and rapid optimization methods can be used, such as the generalized eigenvalue (GenEV) technique (46) or the virtual source method (40). When more flexibility in the formulation of the optimization function is required, genetic algorithms, or variants such as particle swarm optimization, may be used. While genetic algorithms are usually slower and have the disadvantage of potentially not finding a globally optimal configuration, they do tend to find settings less sensitive to antenna steering uncertainties. Exploiting graphical processing units (GPU's), near real-time (10s) optimization using the particle swarm optimization method followed by line-search, was shown to be clinically feasible for effective adaptation to patient complaints (47). Current research is focused towards optimization functions that rely largely on pre-computed information to enable real-time re-optimization (48) or on the use of multi-goal optimization to determine a large number of pareto-optimal settings (49). Both of these approaches can be used to adapt the treatment plan by reweighting different objectives such as tumor temperature, avoidance of regional hotspots, etc.

Errors in the PD predictions must be minimized to avoid sub-optimal clinical outcome and safety issues. Hence, quantitative validation of HTP systems is essential, followed by regular quality assurance (QA) of treatment equipment, e.g. by means of hardware calibrations and regular verification of the heating patterns (5, 6, 32).

Unfortunately, such measurements are time-consuming and costly, so it is common practice to test the validity of the numerical code by comparison to analytical solutions of simple problems. Hence, when choosing appropriate HTP software or solvers, it is of great importance to again validate numerical results against 2D or 3D measurements. These validation measurements should be performed using dedicated phantoms containing well-characterized tissue-simulating materials and accurate, calibrated equipment, such as fiber-optic temperature sensors, infra-red thermography, and electric field sensors (50-52). In addition to phantom measurements, extensive sensitivity studies and (Monte Carlo) uncertainty analyses can be used to assess the impact on HTP predictions of uncertainties in modeling parameters like tissue properties and their age dependence, discretization, and boundary conditions (53).

Recently, EM-HTP is beginning to be used in applications like preplanning-assisted real-time treatment guidance. Since preplanning-optimized treatment settings often cannot avoid treatment-limiting hotspots completely, strategies are under development to convert information such as temperature readings from invasive, intraluminal (54), or non-invasive temperature measurements (55-59) into adjusted settings based on HTP optimization. In addition, objective and reproducible techniques were developed to also exploit subjective information, such as complaints from the patient, into feedback for real-time adjustment of pre-planned settings (60). Effective use of complaint-adaptive steering has been documented in a randomized trial in which clinically evaluated objective measures were applied (61, 62). Recently, the visualizer for electromagnetic dosimetry and optimization (VEDO), a software tool specifically designed to reduce the complexity of SAR-steering, was developed (47,

63). This tool shows how interference patterns between the fields from different antennas, combined with the dielectric inhomogeneity of the human body, result in hotspots, causing patient pain complaints. By displaying the calculated SAR superimposed on CT (or MRI) anatomy information during treatment, VEDO makes it easier to correlate patient complaints to the energy deposition characteristics predicted by the treatment plan. Simulation-based steering with VEDO is currently under clinical investigation for systems with a higher number of antennas and early results, quantified using the mean predicted target SAR and temperature, are promising.

The use of HTP has been very influential in the evaluation and development of new EM applicators (29, 51, 53, 64-67). Furthermore, HTP has been used to study the efficacy of clinical steering guidelines (68) and for the selection of appropriate applicators for specific disease conditions (7).

Ultrasound

HTP based on full-wave 3D simulations is a challenge for HT applications involving US. The small wavelength and the consequent need for high resolution, results in extremely large computational domains, especially for applicators that focus the energy deeply in the body, i.e. which require modeling of a large anatomical region. This makes the application of full-wave 3D simulations cumbersome for US-HTP, especially for array applicators that may have several hundreds of transducers. Therefore careful application-specific approximations are required for reasonable calculation time and accuracy. Alternatively, high performance computing (HPC) techniques for the acceleration of computations, e.g. the use of computer clusters and graphical processing units (GPU), may gradually make full-wave 3D US-HTP more applicable (69). However, to date, US-HTP has been used most frequently to optimize or adapt the aperture of US phased-arrays to the tumor location and/or shape (70-72). Nonetheless, the need for US-HTP is becoming more and more apparent in applications where the small focal volume of the US field produced is inadequate for the larger target volumes. In addition, US-HTP would be valuable in cases where motion-compensation is necessary to handle respiratory motion, or to prevent bone or air interfaces from interfering with the treatment.

Another issue faced by researchers is the lack of reliable tissue acoustic properties, which are necessary to perform realistic and accurate simulations. Although multiple studies were reported over the years (73, 74), the properties have still not been determined for all relevant tissues, frequencies and temperatures and the employed measurement techniques suffer from technical limitations. Also, much of the available measurement data was acquired with what is known as “phase-dependent” experimental techniques, which were later proven to be unreliable (74). Recent studies (75) reported on novel measurement approaches, and measurements on porcine and human samples are currently underway.

US exposure is often characterized in terms of the acoustic field determined under free-field conditions in water, where “free-field” describes circumstances in which the US beam is not affected by boundaries or other obstacles (76). While most human soft tissues have acoustic properties similar to those of water, there are scattering effects at air, fat, and bone interfaces as well as strong absorption in the periosteum of bone. Thus, precise modeling of those tissues is essential for accurate planning. Furthermore, it should be noted that most equations used for numerical modeling of ultrasonic wave propagation (most notably the Westerveld Equation) are derived based on the assumption that thermo-viscous fluids can approximate the modeled media. Consequently, a common simplification in US simulations is to consider only the propagation of longitudinal acoustic waves, while neglecting shear waves, which are non-negligible in hard tissues like bone. A number of studies, however, did show the possibility to accounting for shear waves using the mode conversion technique (77, 78).

Finally, elastic waves in bones are generally not modeled in routine studies of US power deposition in soft tissue, but can be approximated for improved accuracy when the tissue target is near bone (79).

The methods below describe the basic approaches used to compute acoustic waves in soft tissues in order of increasing complexity:

Incident field method: US-HTP tools are most often based on methods that calculate the radiation patterns and transient pressure fields of single transducers and phased arrays in homogeneous media. These methods use point-source superposition (the Rayleigh-Sommerfeld integral), impulse responses for simple geometries, or the fast near-field method (80, 81) to calculate and project the fields produced by simple transducer geometries on planes along the propagation direction.

Angular spectrum method (ASM): This method is a very fast spatial-frequency domain technique derived from Fourier optics (82). A modified version of this method, i.e. “hybrid-SM” (83), can account for effects like attenuation, non-linearity, and even inhomogeneity. These features make ASM ideal for US-HTP, although the method is limited in terms of the transducer geometries it can model and complex wave phenomena like back-scattering and nonlinearity are merely approximated.

Full-wave method: Full-wave propagation generally uses integral equations to predict full-wave propagation, absorption, and temperature distributions in tissue. Generally it fully accounts for all effects of acoustic and thermal heterogeneities (84). However, full-wave treatment planning is still limited to specific applications and frequency ranges, since enormous computational resources are required for sufficiently fine discretization with respect to the wavelength. Although computationally expensive, full-wave methods provide the most accurate predictions for HTP (Figure 2).

Freely available software include Field II (Impulse response) (85), the faster Focus (Fast Near-field Method and ASM) (86, 87) and k-wave (ASM) (88, 89).

Despite the innate need for optimization of pressure fields, little progress has been made in the area of optimization of US PD in tissue. Although theoretically possible (90), the large number of elements typically in therapeutic US transducer arrays, i.e. up to 1024, combined with the need for enormous computational resources for full-wave simulations, render most patient-specific optimization techniques impractical. However, the use of incident-field methods, dramatically reduces the computational cost, and applications of US-HTP with numerically computed phase-corrections have been reported (91-93). Such a case is liver ablation where optimization is necessary in order to minimize the ribcage scattering (intercostal space targeting). Modeling was used to generate a focus in a target partly obscured by ribs (94).

Validation in US-HTP is typically limited to that of the different numerical software approaches used to calculate the predicted acoustic and thermal energy depositions. In terms of validating US solvers, a number of approaches, ranging from analytical validation against pre-computed fields to comparison against measured US fields in water-tank setups, have been used. Usually the pressure and temperature generated by actual transducers in the presence of acoustically characterized tissue (skull (95, 96) and bovine femur(97-99)), man-made samples (100, 101), or phantoms (102), was measured using movable hydrophone and/or thermocouples and compared to numerical results. However, to date, no comprehensive validation of the entire US-HTP procedure has been presented, and the efficacy of the treatment is usually evaluated by online monitoring of the induced temperature increase and/or radiation force (103-105).

In clinical hyperthermia applications, US-HTP is typically used with incident-field US solvers to optimize the steering parameters of the transducer elements to maximize thermal dose in the target volume. US and MR imaging are often combined to image and control the position of the US beam focus during heating. In this setting, US-HTP is applied to adjust settings such that underexposed regions also get heated, e.g. by scanning the focus and dynamically covering the entire target volume. Input parameters for planning specify the US transducer (array) geometries, dimensions and positions, the focal length and diameter of each transducer, and tissue geometry (anatomy), boundary conditions, interfaces, and properties. With this input, the radiation pattern of the transducer array is then optimized, usually with incident-field-based simulations to obtain the desired depth, shape, and/or trajectory of heating (76).

Moros *et al.* used US-HTP to develop the SURLAS applicator (106) and to assess the impact of having bone (ribs) in the ultrasound beam path (79, 107). Regarding US-HTP, they concluded that improvements in accuracy and especially calculation speed are required to facilitate more-routine clinical application (108).

For interstitial and catheter-based heating approaches, with even higher US frequencies used, the resolution required for accurate thermal and SAR modeling close to the device is even more stringent than for physically larger external transducers, due to smaller wavelengths, more localized heating and high thermal gradients. Nevertheless, the feasibility and accuracy of HTP for these applications have been demonstrated in both interstitial (109) and intraluminal (110) applications. The UCSF research team also used HTP to establish guidelines that restrict pelvic bone heating during prostate thermal therapy (111).

Temperature Distribution Simulation Techniques

While SAR modeling is maturing rapidly, the accuracy of temperature predictions is lagging behind. This is due to large uncertainties in the thermal properties of tissue, which vary between patients, within the patient, within each tissue, over time, and as a non-linear function of tissue temperature. The variation with time is even more pronounced with varying temperature (spatially and temporally) due to the nonlinear and patient-specific physiological response of thermoregulation. The spacing of thermally significant blood vessels is heterogeneous, affected by tumor growth and changes with both temperature and thermal dose. Thus, an accurate 3D prediction of the thermal tissue properties is an extreme challenge. The discrete vasculature (DIVA) model (112) considers the impact of individual vessels. Currently, however, devising even a moderately detailed vascular tree can take up to a month of man hours. Thus, the method most commonly used to model heat transfer in living tissue is the PBHE (113), a continuum model that models the impact of perfusion as an isotropic heat sink. Mathematically, it is expressed as:

$$\rho c\frac{\partial T}{\partial t}=\nabla\cdot(k\nabla T)+\rho Q+\rho S-\rho_b c_b\rho\omega(T-T_b),$$

where T is the temperature, t is the time, ρ is the volume density of mass, c is the specific heat capacity, k is the thermal conductivity, ω is the volumetric blood perfusion rate, Q is the metabolic heat generation rate, S is the specific absorption rate (SAR), and the subscript b denotes a blood property. For clarity, we omitted the parameter dependencies on T, t and spatial position r. This model includes heat conduction in tissue and accounts for energy inputs from metabolism (Q) and external power sources (S). Note that computations of the SAR and temperature modeling are usually decoupled, to reduce the complexity and computational requirements. The last part of the equation accounts for convective cooling by

blood perfusion, which is assumed to be non-directional, thus, heat disappears from the tissue via a non-directional heat-sink term. For modeling a regional temperature distribution in tissue with healthy microvasculature and blood flowing through vessels with isotropically distributed orientations, the validity of this equation has been demonstrated. However, for accurate modeling of the impact of blood vessels with dimensions exceeding 0.2mm diameter on the local tissue temperature, the directional effects of blood flow cannot be ignored (114). Many numerical implementations of the PBHE exist, but the most common method is based on the finite difference time domain (FDTD) method (115). Boundary conditions are used to account for convective or sweating heat loss at the patient surface. In some implementations, the temperature dependence of tissue parameters (especially perfusion) is considered, and models that permit body core heating via an increasing blood temperature exist (116)

To capture directional heat flow through tissue, various models have been developed, including the addition of convective terms (117, 118), tensorial effective conductivity (117, 118) and discrete vasculature (DIVA) models (112). The latter have been developed to take into account the non-continuum nature of perfusion and non-equilibrium effects. Thermally significant vasculature is modeled, taking into account vessel size as well as velocity and direction of blood flow (3, 119-122). In DIVA models, a realistic vessel tree is obtained from imaging, e.g. using MRI, and included in the thermal model. One problem is this produces at best a snapshot of the vasculature at the time of imaging, whereas vessel size varies in time and temperature. Another problem of DIVA models is that generation of a vessel tree is a tedious procedure that involves many manual interactions and approximations (3). In addition, only vessels 0.6mm diameter and larger can currently be identified with MRI (123), whereas heat exchange is thermally significant in vessels down to 0.2mm diameter. Therefore, attempts have been made to generate artificial vessels (112, 124-126)}, and Craciunescu et al (127) investigated ways to combine vessel tree data with perfusion maps to include heterogeneous perfusion on a micro scale.

Regardless of how accurately the blood vessel tree is modeled prior to heating, static PBHE and DIVA models are only approximate, since blood vessel size and perfusion rates change dramatically as a function of temperature and duration of heating. Several groups have demonstrated changes in tissue blood perfusion of over 10 times during heating in the 40–45°C range (128-131). Therefore, amendments to the PBHE that incorporate the significantly temperature-dependent nonlinear effects on thermal tissue characteristics have been proposed. The simplest example is to incorporate temperature dependent parameters (13). Another example of an amended PBHE model is the use of mixed models that incorporate effective conductivity (2, 132). In these models, the tissue dependent conductivity k from the PBHE is replaced by $k_{eff} = k(1 + C\omega)$, where ω denotes perfusion and C is an empirical factor that must be experimentally assessed for each application and per tissue. Other thermal models treat arterial and venous blood temperature as spatially and temporally variable. An overview of these models is provided by Arkin et al (117).

At this time, variations of the PBHE method are generally used for thermal modeling of clinical applications because they: 1) lead to reasonable estimates within the known uncertainty of tissue properties; and 2) can be applied without inclusion of accurate vascular trees, which are computationally unmanageable for large tissue regions. However, thermal predictions are very sensitive to thermal parameters, and little data is available on these properties or their variation between patients and under heat stress. Therefore, an extensive uncertainty evaluation per application and treatment site is essential to quantify the accuracy of patient-specific predictions. A Monte-Carlo uncertainty analysis is a valuable tool for addressing this uncertainty due to the strong correlation between thermal parameters. The IT'IS database (133) provides the thermal parameters for the PBHE of many tissues, as well

as the variation of the values reported in literature. This information can be used as input for rigorous uncertainty assessments aimed at understanding the resulting variation in PD and temperature distributions, as is the current standard in EM dosimetry (134).

Several investigators have studied the use of thermal modeling to optimize phase and amplitude, i.e. the electronic steering parameters of phased-array applicators (40, 41, 44). Most often, the approach is based on optimization of EM power deposition performed prior to calculation of the resulting temperature distribution. When nonlinear thermal models are used, e.g. to consider thermoregulation, often the optimization includes numerically expensive repeated simulations. Alternatively, more advanced approaches permit the optimization and thermal modeling problem to be solved in a combined approach, e.g. using the partial differential equation (PDE) constraint interior point optimization (9, 10).

Although validation in phantoms has been performed successfully, continued progress in clinical validation of temperature treatment planning is required. In patients, validation of thermal models has traditionally been performed by means of invasive and intraluminal temperature measurements. Unfortunately, these methods are cumbersome, can lead to complications, and provide information only for a small number of locations. The development of MR hybrid hyperthermia systems with thermal imaging capability has opened the door to acquisition of thermal tissue properties during heating (135) and validation of preplanned SAR (67) and temperature profiles (58). However, since only a limited number of such hybrid systems are currently available, it will take time before real-time treatment planning re-optimization based on thermal simulations has matured sufficiently to be accepted for clinical hyperthermia treatments.

Although thermal models have limitations for accurate prediction of temperature distributions in heterogeneous perfused tissue, there are numerous applications that can benefit from thermal modeling. Certainly, thermal models are an excellent tool for best- and worst-case scenario analyses (136). In addition, they can be used to intelligently interpolate temperatures between sparsely measured points. Thermal modeling has also been used successfully to study the influence of water bolus cooling on expected temperature distributions of superficial heat applicators (137-140) and to investigate the influence of uncertainties in thermal parameters on applicator choice for deep-regional hyperthermia (24, 53, 141). With continued development, temperature modeling is expected to become useful for prediction of thermal dose and treatment outcome.

Dose concepts and HT optimization

Defining an optimization function with clinical relevance for the combined treatment of HT with other treatment modalities like radiotherapy and chemotherapy, is not straightforward, due to the multiple interaction mechanisms involved. Thermal optimization can aim at one or more of the following goals: to achieve a target temperature distribution, to optimize heating of tumor compared to healthy tissue, avoidance of hotspots, and maximized tumor coverage. In some cases, rather than temperature, thermal dose quantities are optimized, e.g., CEM43°C (thermal iso-effect dose) (142), which is similar to an “Arrhenius relationship”. This formulation has been shown to correlate with outcome in clinical trials, although it was derived from rodent studies for thermal damage only (143-145).

To reduce the influence of outliers, clinical temperatures are often expressed in terms of percentile ranking. The T50, for example, indicates that 50% of measured points exceed a given temperature value, i.e. the median temperature. When the time of heating is taken into account, parameters such as the CEM43°C T90, which converts the temperature-time profile of any given heating session into the equivalent number of minutes for which 90% of the tumor exceeds 43°C, may be calculated.

An alternative concept is the TRISE parameter introduced by Franckena et al. (146). This parameter specifies the increment of T50 that was measured, averaged over all treatments and intended minutes of total treatment time actually delivered. In a clinical trial with 420 patients treated for locally advanced cervical cancer (LACC), TRISE correlated with both tumor control and survival, whereas CEM43T90 correlated only with survival (146).

Although research that considers the transient nature of heating has been performed, typically only the steady-state temperature distribution, e.g. the mean target temperature, is optimized in current HTP. It should be noted that uncertainties in thermal tissue properties can severely restrict the improvement possible from thermal optimizations, as compared to possible benefits from PD optimization, using e.g. the hotspot target coefficient (HTQ) (8, 53). Furthermore, PD-related indicators such as, i.e., the 25% or 50% of the maximum iso-SAR coverage over the target region, also have been shown to correlate with clinical outcome (147). Hence, although temperature-based dose concepts provide the most promising approaches for optimization goals, using temperature-based optimization is still the topic of debate (148).

Commercial treatment planning packages

The last two decades have witnessed a shift in emphasis from development of modeling algorithms and simulation software approaches to the use of high-level integrated multi-physics HTP programs and systems for applicator design and clinical treatment planning. Non-commercial programs have been developed by groups such as the University Medical Center Utrecht (3), the University of California San Francisco (109, 149), and Duke University (150) in planning for specific applicators and treatment sites.

The most widely used commercial HTP system is Sigma-HyperPlan, which was specifically designed for deep hyperthermia with the BSD2000 system (151) (Dr. Sennewald Medizintechnik GmbH, Munich Germany). Sigma-HyperPlan was developed at the Konrad Zuse Institute (28) and has been evaluated for clinical use at the Charite Klinikum (15, 55, 148, 152), Erasmus MC (34, 60, 62, 68, 153), and Duke University (154). Figure 3 shows the PD (top row) and temperature (bottom row) distributions predicted by Sigma-HyperPlan for patients of different dimensions using the same applied power and phase parameters, and with the same maximum temperature in normal tissue (bottom row). Clearly, patient-anatomy largely influences the distributions obtained during deep HT, and hence patient-specific modeling is required. In addition, large differences between PD and temperature distributions are found in this theoretical study, which advocates the use of temperature-based optimization.

In the last decade, a second commercial HTP package was developed, based on SEMCAD X (SPEAG, Zurich, Switzerland) and introduced by the Erasmus MC group for clinical planning of superficial HT (7) and deep HT (51). SEMCAD X, originally developed as a software tool for high-resolution EM simulations involving complex anatomical models, allows creation and analysis of various applicator models. Addition of the segmentation tool iSEG (www.zurichmedtech.com), multiple thermal solvers (PBHE, keff, DIVA), and several SAR and temperature optimization approaches as well as post-processing routines for dose and effect quantification has elevated SEMCAD X to a flexible HTP framework. Recently, a third integrated HTP package, i.e. ALBA HTPS (www.albahyperthermia.com), has become available. This package is based on the EM and thermal kernels of the CST multi-physics simulator (www.cst.com) and was developed in cooperation with the University of Rome Tor Vergata. Finally, although not integrated HTP platforms, COMSOL (www.comsol.com) and HFSS (www.ansys.com) provide most of the simulation functionality required for HTP when combined with separate programs for tissue segmentation. For HFSS, Duke University

showed that integration of commercial segmentation and EM and a thermal solver with MR based thermometry enables optimization of HT quality (Figure 4) (155). In this study, they demonstrated that a pre-treatment plan could be significantly optimized, within minutes, using on the basis of real-time temperature monitoring feedback.

Outlook/Discussion

In recent years, HTP has begun to emerge into practical clinical use. The main strength of simulations is that the effectiveness of different scenarios can be judged before the HT session to aid in selection of patient, applicator or treatment approach, specific power excitation planning, and clinical outcome prediction. In addition, simulations are helpful for assessing treatment risks to the patient, e.g. effect of metallic implants, or operator. HTP simulation tools can be used to develop enhanced treatment approaches or, retrospectively, to analyze treatment quality. Other areas where HTP tools play an important role are the education and training of hyperthermia technicians and physicians, treatment visualization, development of QA guidelines and protocols, and basic research to increase understanding of hyperthermia treatments or assess related uncertainties and the impact of individual parameters. In our experience, treatment plans provide an objective basis for stimulating interdisciplinary discussions and as well as an excellent venue for continuous training and improvement in therapy.

For the future, we expect that thermal modeling will continue to mature and will be used to prospectively compare treatment options, optimize treatments as well as to enrich temperature measurement data. In treatments where non-invasive measurement of 2D and 3D thermal distributions is possible, HTP models will be complemented with fast optimization feedback control algorithms that can correct for model errors and uncertainties (39-41, 156). For treatments where MR thermal imaging is not a realistic option, thermal models are even more critical for improving treatment quality. Due to the overlapping and complementary information obtained, further innovation of prospective PD and thermal modeling should go hand-in-hand with development of non-invasive thermometry approaches. In vivo validation of the developed HTP tools and assessment of the offered benefit will be of critical importance going forward, as will be the development of tools that are suitably embedded in the clinical work-flow for routine clinical use.

Conclusions

HTP has demonstrated major progress over the past decade and is rapidly gaining ground in practical clinical application. Even when its limitations and ongoing development are considered, HTP in its current form is already improving treatment quality. HTP has demonstrated its usefulness in the design of new heating equipment, in providing critical understanding of the relative role of multiple conflicting treatment parameters, in guiding the development of updated treatment protocols, and in the education and training of technologists and physicians. Finally, the advent of non-invasive measurement strategies is expected to be a strong stimulant for improved accuracy of patient-specific simulations and real-time treatment optimization strategies.

Acknowledgments

The authors of Erasmus MC are financially supported by the Dutch Cancer Society and Technology Foundation STW, the authors of Duke University hospital by NIH (grant PO1-CA42745), and IT'IS gratefully acknowledges CTI (8059.2 LSPP-LS) and CO-ME.

References

1. van der Zee J. Heating the patient: a promising approach? Ann Oncol. 2002 Aug; 13(8):1173–84. [PubMed: 12181239]
2. Lagendijk, JJW.; Van den Berg, PM.; Bach Andersen, J.; Hand, JW.; Bardati, F.; Uzunoglu, NK., et al., editors. Treatment planning and modelling in hyperthermia: a task group report. Rome: Tor Vergata, Postgraduate School of Medical Physics, II Universiy of Rome; 1992.
3. Lagendijk JJ. Hyperthermia treatment planning. Phys Med Biol. 2000 May; 45(5):R61–76. [PubMed: 10843091]
4. Wissler EH. Pennes' 1948 paper revisited. J Appl Physiol. 1998 Jul; 85(1):35–41. [PubMed: 9655751]
5. Bruggmoser G. Some aspects of quality management in deep regional hyperthermia. Int J Hyperthermia. 2012; 28(6):562–9. [PubMed: 22857615]
6. Bruggmoser G, Bauchowitz S, Canters R, Crezee H, Ehmann M, Gellermann J, et al. Guideline for the clinical application, documentation and analysis of clinical studies for regional deep hyperthermia: quality management in regional deep hyperthermia. Strahlenther Onkol. 2012 Sep; 188(2):198–211. [PubMed: 22926657]
7. de Bruijne M, Wielheesen DH, van der Zee J, Chavannes N, van Rhoon GC. Benefits of superficial hyperthermia treatment planning: five case studies. Int J Hyperthermia. 2007 Aug; 23(5):417–29. [PubMed: 17701533]
8. Canters RA, Wust P, Bakker JF, Van Rhoon GC. A literature survey on indicators for characterisation and optimisation of SAR distributions in deep hyperthermia, a plea for standardisation. Int J Hyperthermia. 2009 Nov; 25(7):593–608. [PubMed: 19848621]
9. Weiser, M.; Schiela, A. Function space interior point methods for PDE constrained optimization. Zuse Institute Berlin; 2004.
10. Christen, M.; Schenk, O.; Burkhart, H. Large-Scale PDE-constrained Optimization in Hyperthermia Cancer Treatment Planning; SIAM Conference on Parallel Processing for Scientific Computung; Atlanta, US. 2008;
11. Wust P, Gellermann J, Beier J, Wegner S, Tilly W, Troger J, et al. Evaluation of segmentation algorithms for generation of patient models in radiofrequency hyperthermia. Phys Med Biol. 1998 Nov; 43(11):3295–307. [PubMed: 9832017]
12. Paulides MM, Bakker JF, Linthorst M, van der Zee J, Rijnen Z, Neufeld E, et al. The clinical feasibility of deep hyperthermia treatment in the head and neck: new challenges for positioning and temperature measurement. Phys Med Biol. 2010 May 7; 55(9):2465–80. [PubMed: 20371911]
13. Lang J, Erdmann B, Seebass M. Impact of nonlinear heat transfer on temperature control in regional hyperthermia. IEEE Trans Biomed Eng. 1999 Sep; 46(9):1129–38. [PubMed: 10493076]
14. Wust P, Nadobny J, Seebass M, Stalling D, Gellermann J, Hege HC, et al. Influence of patient models and numerical methods on predicted power deposition patterns. Int J Hyperthermia. 1999 Nov-Dec;15(6):519–40. [PubMed: 10598949]
15. Gellermann J, Wust P, Stalling D, Seebass M, Nadobny J, Beck R, et al. Clinical evaluation and verification of the hyperthermia treatment planning system hyperplan. Int J Radiat Oncol Biol Phys. 2000 Jul 1; 47(4):1145–56. [PubMed: 10863088]
16. Farace P, Pontalti R, Cristoforetti L, Antolini R, Scarpa M. An automated method for mapping human tissue permittivities by MRI in hyperthermia treatment planning. Phys Med Biol. 1997 Nov; 42(11):2159–74. [PubMed: 9394404]
17. Mazzurana M, Sandrini L, Vaccari A, Malacarne C, Cristoforetti L, Pontalti R. A semi-automatic method for developing an anthropomorphic numerical model of dielectric anatomy by MRI. Phys Med Biol. 2003 Oct 7; 48(19):3157–70. [PubMed: 14579858]
18. Gabriel C, Gabriel S, Corthout E. The dielectric properties of biological tissues: I. Literature survey. Physics in Medicine and Biology. 1996; 41(11):2231–49. [PubMed: 8938024]
19. Gabriel S, Lau RW, Gabriel C. The dielectric properties of biological tissues: II. Measurements in the frequency range 10 Hz to 20 GHz. Physics in Medicine and Biology. 1996; 41(11):2251–69. [PubMed: 8938025]

20. Surowiec AJ, Stuchly SS, Barr JB, Swarup A. Dielectric properties of breast carcinoma and the surrounding tissues. IEEE Trans Biomed Eng. 1988 Apr; 35(4):257–63. [PubMed: 2834285]
21. Zastrow E, Davis SK, Lazebnik M, Kelcz F, Van Veen BD, Hagness SC. Development of anatomically realistic numerical breast phantoms with accurate dielectric properties for modeling microwave interactions with the human breast. IEEE Trans Biomed Eng. 2008 Dec; 55(12):2792–800. [PubMed: 19126460]
22. van Lier AL, Brunner DO, Pruessmann KP, Klomp DW, Luijten PR, Lagendijk JJ, et al. B1(+) phase mapping at 7 T and its application for in vivo electrical conductivity mapping. Magn Reson Med. 2012 Feb; 67(2):552–61. [PubMed: 21710613]
23. Van de Kamer JB, Van Wieringen N, De Leeuw AA, Lagendijk JJ. The significance of accurate dielectric tissue data for hyperthermia treatment planning. Int J Hyperthermia. 2001; 17(2):123–42. [PubMed: 11252357]
24. De Greef M, Kok HP, Correia D, Borsboom PP, Bel A, Crezee J. Uncertainty in hyperthermia treatment planning: the need for robust system design. Phys Med Biol. 2011 Jun 7; 56(11):3233–50. [PubMed: 21540493]
25. Fortunati, V.; Verhaart, RF.; Van der Lijn, F.; Niessen, WJ.; Veenland, JF.; Paulides, MM., et al. Hyperthermia critical tissues automatic segmentation of head and neck CT images using atlas registration and graph cuts. IEEE-ISBI; 5th Barcelona: May 2nd. 2012
26. Fortunati V, Verhaart RF, Van der Lijn F, Niessen WJ, Veenland JF, Paulides MM, et al. Tissue segmentation of head and neck CT images for treatment planning: a multi-atlas approach combined with intensity modeling. Med Phys. accepted;-(-).
27. Hand JW. Modelling the interaction of electromagnetic fields (10 MHz-10 GHz) with the human body: methods and applications. Phys Med Biol. 2008 Aug 21; 53(16):243–86.
28. Deuflhard P, Schiela A, Weiser M. Mathematical cancer therapy planning in deep regional hyperthermia. Acta Numerica. 2012; 21:307–78.
29. de Bruijne M, Samaras T, Chavannes N, van Rhoon GC. Quantitative validation of the 3D SAR profile of hyperthermia applicators using the gamma method. Phys Med Biol. 2007 Jun 7; 52(11): 3075–88. [PubMed: 17505090]
30. Raskmark P, Larsen T, Hornsleth SN. Multi-applicator hyperthermia system description using scattering parameters. Int J Hyperthermia. 1994; 10(1):143–51. [PubMed: 8144985]
31. Wust P, Fahling H, Helzel T, Kniephoff M, Wlodarczyk W, Monich G, et al. Design and test of a new multi-amplifier system with phase and amplitude control. Int J Hyperthermia. 1998; 14(5): 459–77. [PubMed: 9789770]
32. Bakker JF, Paulides MM, Westra AH, Schippers H, Van Rhoon GC. Design and test of a 434 MHz multi-channel amplifier system for targeted hyperthermia applicators. Int J Hyperthermia. 2010; 26(2):158–70. [PubMed: 20146570]
33. Trefna HD, Togni P, Shiee R, Vrba J, Persson M. Design of a wideband multi-channel system for time reversal hyperthermia. Int J Hyperthermia. 2012; 28(2):175–83. [PubMed: 22335231]
34. Canters RA, Franckena M, Paulides MM, Van Rhoon GC. Patient positioning in deep hyperthermia: influences of inaccuracies, signal correction possibilities and optimization potential. Phys Med Biol. 2009; 54(12):3923–36. [PubMed: 19491453]
35. de Bruijne M, Samaras T, Bakker JF, van Rhoon GC. Effects of waterbolus size, shape and configuration on the SAR distribution pattern of the Lucite cone applicator. Int J Hyperthermia. 2006; 22(1):15–28. [PubMed: 16423750]
36. Correia D, Kok HP, de Greef M, Bel A, van Wieringen N, Crezee J. Body conformal antennas for superficial hyperthermia: the impact of bending contact flexible microstrip applicators on their electromagnetic behavior. IEEE Trans Biomed Eng. 2009; 56(12):2917–26. [PubMed: 19695983]
37. Wust P, Seebass M, Nadobny J, Deuflhard P, Monich G, Felix R. Simulation studies promote technological development of radiofrequency phased array hyperthermia. 1996. Int J Hyperthermia. 2009; 25(7):517–28. [PubMed: 19848614]
38. Bardati F, Borrani A, Gerardino A, Lovisolo GA. SAR optimization in a phased array radiofrequency hyperthermia system. Specific absorption rate. IEEE Trans Biomed Eng. 1995; 42(12):1201–7. [PubMed: 8550062]

39. Cheng KS, Stakhursky V, Stauffer P, Dewhirst M, Das SK. Online feedback focusing algorithm for hyperthermia cancer treatment. Int J Hyperthermia. 2007 Nov; 23(7):539–54. [PubMed: 17943551]
40. Cheng KS, Stakhursky V, Craciunescu OI, Stauffer P, Dewhirst M, Das SK. Fast temperature optimization of multi-source hyperthermia applicators with reduced-order modeling of 'virtual sources'. Phys Med Biol. 2008 Mar 21; 53(6):1619–35. [PubMed: 18367792]
41. Cheng KS, Yuan Y, Li Z, Stauffer PR, Maccarini P, Joines WT, et al. The performance of a reduced-order adaptive controller when used in multi-antenna hyperthermia treatments with nonlinear temperature-dependent perfusion. Phys Med Biol. 2009 Mar 5; 54(7):1979–95. [PubMed: 19265209]
42. Cheng, K.; Yuan, Y.; Li, Z.; Stauffer, P.; Joines, W.; Dewhirst, M., et al., editors. Proc Of SPIE. San Jose: SPIE Press; Bellingham WA: 2009. Control time reduction using virtual source projection for treating a leg sarcoma with nonlinear perfusion.
43. Das SK, Clegg ST, Samulski TV. Electromagnetic thermal therapy power optimization for multiple source applicators. Int J Hyperthermia. 1999 Jul-Aug;15(4):291–308. [PubMed: 10458569]
44. Kok HP, Van Haaren PM, Van de Kamer JB, Wiersma J, Van Dijk JD, Crezee J. High-resolution temperature-based optimization for hyperthermia treatment planning. Phys Med Biol. 2005 Jul 7; 50(13):3127–41. [PubMed: 15972985]
45. Kok HP, van Haaren PM, van de Kamer JB, Zum Vorde Sive Vording PJ, Wiersma J, Hulshof MC, et al. Prospective treatment planning to improve locoregional hyperthermia for oesophageal cancer. Int J Hyperthermia. 2006 Aug; 22(5):375–89. [PubMed: 16891240]
46. Kohler T, Maass P, Wust P, Seebass M. A fast algorithm to find optimal controls of multiantenna applicators in regional hyperthermia. Phys Med Biol. 2001 Sep; 46(9):2503–14. [PubMed: 11580185]
47. Rijnen Z, van Rhoon GC, Bakker JF, Canters RAM, Togni P, Paulides MM. Introducing VEDO for complaint adaptive hyperthermia in the head and neck. Int J Hyperthermia. accepted.
48. Neufeld, E.; Chavannes, N.; Paulides, MM.; Van Rhoon, GC.; Kuster, N. Fast (re-)optimization for hyperthermia: Bringing treatment planning into the treatment room. 10th International Congress on Hyperthermic Oncology; Munich, Germany. 2008;
49. Jain RK, Grantham FH, Gullino PM. Blood flow and heat transfer in Walker 256 mammary carcinoma. J Natl Cancer Inst. 1979; 62(4):927–33. [PubMed: 285296]
50. Paulides MM, Bakker JF, van Rhoon GC. Electromagnetic head-and-neck hyperthermia applicator: experimental phantom verification and FDTD model. Int J Radiat Oncol Biol Phys. 2007 Jun 1; 68(2):612–20. [PubMed: 17418965]
51. Paulides MM, Bakker JF, Neufeld E, van der Zee J, Jansen PP, Levendag PC, et al. The HYPERcollar: a novel applicator for hyperthermia in the head and neck. Int J Hyperthermia. 2007 Nov; 23(7):567–76. [PubMed: 18038287]
52. Fatehi D, van Rhoon GC. SAR characteristics of the Sigma-60-Ellipse applicator. Int J Hyperthermia. 2008 Jun; 24(4):347–56. [PubMed: 18465419]
53. Canters RA, Paulides MM, Franckena M, Mens JW, van Rhoon GC. Benefit of replacing the Sigma-60 by the Sigma-Eye applicator: A Monte Carlo-based uncertainty analysis. Strahlenther Onkol. 2013 Jan; 189(1):74–80. [PubMed: 23161121]
54. Fatehi D, van der Zee J, Notenboom A, van Rhoon GC. Comparison of intratumor and intraluminal temperatures during locoregional deep hyperthermia of pelvic tumors. Strahlenther Onkol. 2007 Sep; 183(9):479–86. [PubMed: 17762921]
55. Gellermann J, Weihrauch M, Cho CH, Wlodarczyk W, Fahling H, Felix R, et al. Comparison of MR-thermography and planning calculations in phantoms. Med Phys. 2006 Oct; 33(10):3912–20. [PubMed: 17089853]
56. Stauffer, PR.; Craciunescu, OI.; Maccarini, PF.; Arunachalam, K.; Arabe, O.; Stakhursky, V., et al., editors. Proceedings of SPIE. San Jose: SPIE Press; 2009. Clinical utility of magnetic resonance thermal imaging (MRTI) for realtime guidance of deep hyperthermia.

57. Weihrauch M, Wust P, Weiser M, Nadobny J, Eisenhardt S, Budach V, et al. Adaptation of antenna profiles for control of MR guided hyperthermia (HT) in a hybrid MR-HT system. Med Phys. 2007 Dec; 34(12):4717–25. [PubMed: 18196799]
58. Gellermann J, Hildebrandt B, Issels R, Ganter H, Wlodarczyk W, Budach V, et al. Noninvasive magnetic resonance thermography of soft tissue sarcomas during regional hyperthermia: correlation with response and direct thermometry. Cancer. 2006 Sep 15; 107(6):1373–82. [PubMed: 16902986]
59. Craciunescu O, Stauffer P, Soher B, Maccarini P, Das S, Cheng K, et al. Accuracy of real time noninvasive temperature measurements using magnetic resonance thermal imaging in patients treated for high grade extremity soft tissue sarcomas. Medical Physics. 2009; 36(11):4848–58. [PubMed: 19994492]
60. Canters RA, Franckena M, van der Zee J, van Rhoon GC. Optimizing deep hyperthermia treatments: are locations of patient pain complaints correlated with modelled SAR peak locations? Phys Med Biol. 2011 Jan 21; 56(2):439–51. [PubMed: 21178235]
61. Franckena M, Lutgens LC, Koper PC, Kleynen CE, van der Steen-Banasik EM, Jobsen JJ, et al. Radiotherapy and hyperthermia for treatment of primary locally advanced cervix cancer: results in 378 patients. Int J Radiat Oncol Biol Phys. 2009 Jan 1; 73(1):242–50. [PubMed: 18990505]
62. Franckena M, Canters R, Termorshuizen F, Van Der Zee J, Van Rhoon G. Clinical implementation of hyperthermia treatment planning guided steering: A cross over trial to assess its current contribution to treatment quality. Int J Hyperthermia. 2010; 26(2):145–57. [PubMed: 20146569]
63. Canters RA, Paulides MM, Franckena MF, van der Zee J, van Rhoon GC. Implementation of treatment planning in the routine clinical procedure of regional hyperthermia treatment of cervical cancer: an overview and the Rotterdam experience. Int J Hyperthermia. 2012; 28(6):570–81. [PubMed: 22690757]
64. Seebass M, Beck R, Gellermann J, Nadobny J, Wust P. Electromagnetic phased arrays for regional hyperthermia: optimal frequency and antenna arrangement. Int J Hyperthermia. 2001 Jul-Aug; 17(4):321–36. [PubMed: 11471983]
65. De Greef M, Kok HP, Bel A, Crezee J. 3D versus 2D steering in patient anatomies: a comparison using hyperthermia treatment planning. Int J Hyperthermia. 2011; 27(1):74–85. [PubMed: 21204620]
66. Dobsicek Trefna H, Vrba J, Persson M. Evaluation of a patch antenna applicator for time reversal hyperthemia. Int J Hyperthermia. 2010; 26(2):185–97. [PubMed: 20146572]
67. Li Z, Vogel M, Maccarini P, Stakhursky V, Soher B, Craciunescu O, et al. Improved hyperthermia treatment control using SAR/temperature simulation and PRFS magnetic resonance thermal imaging. Int J Hyperthermia. 2011; 27(1):86–99. [PubMed: 21070140]
68. van der Wal E, Franckena M, Wielheesen DH, van der Zee J, van Rhoon GC. Steering in locoregional deep hyperthermia: evaluation of common practice with 3D-planning. Int J Hyperthermia. 2008 Dec; 24(8):682–93. [PubMed: 19065346]
69. Hlawitschka M, McGough RJ, Ferrara KW, Kruse DE. Fast ultrasound beam prediction for linear and regular two-dimensional arrays. IEEE Trans Ultrason Ferroelectr Freq Control. 2011 Sep; 58(9):2001–12. [PubMed: 21937338]
70. McGough RJ, Kessler ML, Ebbini ES, Cain CA. Treatment planning for hyperthermia with ultrasound phased arrays. IEEE Transactions on Ultrasonics, Ferroelectrics and Frequency Control. 1996; 43(6):1074–84.
71. Nikolov SI, Jensen JA. Application of different spatial sampling patterns for sparse array transducer design. Ultrasonics. 2000 Jul; 37(10):667–71. [PubMed: 10950348]
72. Chen D, Xia R, Chen X, Shafirstein G, Corry PM, Griffin RJ, et al. SonoKnife: feasibility of a line-focused ultrasound device for thermal ablation therapy. Med Phys. 2011 Jul; 38(7):4372–85. [PubMed: 21859038]
73. Duck, FA. Physical properties of tissue: a comprehensive reference book. Academic Pr; 1990.
74. Nyborg, W.; Carson, P.; Dunn, F. Biological effects of ultrasound: meachnisms and clinical implications. 1983. Report No.: 0913392642

75. El-Brawany M, Nassiri D, Terhaar G, Shaw A, Rivens I, Lozhken K. Measurement of thermal and ultrasonic properties of some biological tissues. Journal of Medical Engineering & Technology. 2009; 33(3):249–56. [PubMed: 19340696]
76. Haar GT, Coussios C. High intensity focused ultrasound: physical principles and devices. Int J Hyperthermia. 2007 Mar; 23(2):89–104. [PubMed: 17578335]
77. Mast TD, Hinkelman LM, Orr MJ, Sparrow VW, Waag RC. Simulation of ultrasonic pulse propagation through the abdominal wall. The Journal of the Acoustical Society of America. 1997; 102:1177. [PubMed: 9265762]
78. White P, Clement G, Hynynen K. Longitudinal and shear mode ultrasound propagation in human skull bone. Ultrasound in medicine & biology. 2006; 32(7):1085–96. [PubMed: 16829322]
79. Moros EG, Straube WL, Myerson RJ, Fan X. The impact of ultrasonic parameters on chest wall hyperthermia. Int J Hyperthermia. 2000 Nov-Dec;16(6):523–38. [PubMed: 11129263]
80. McGough RJ, Samulski TV, Kelly JF. An efficient grid sectoring method for calculations of the near-field pressure generated by a circular piston. Journal of the Acoustical Society of America. 2004 May; 115(5):1942–54. [PubMed: 15139603]
81. Chen D, Kelly JF, McGough RJ. A fast near-field method for calculations of time-harmonic and transient pressures produced by triangular pistons. J Acoust Soc Am. 2006 Nov; 120(5 part 1): 2450–9. [PubMed: 17139708]
82. Goodman J, Gustafson S. Introduction to Fourier Optics, Second Edition. Opt Eng. 1996; 35(5): 1513.
83. Vyas U, Christensen D. Ultrasound beam simulations in inhomogeneous tissue geometries using the hybrid angular spectrum method. IIEEE Trans Ultrason Ferroelectr Freq Control. 2012; 59(6): 1093–100.
84. Bakker JF, Paulides MM, Obdeijn IM, van Rhoon GC, van Dongen KW. An ultrasound cylindrical phased array for deep heating in the breast: theoretical design using heterogeneous models. Phys Med Biol. 2009 May 21; 54(10):3201–15. [PubMed: 19420416]
85. Jensen JA, Svendsen NB. Calculation of pressure fields from arbitrarily shaped, apodized, and excited ultrasound transducers. IEEE Trans Ultrason Ferroelectr Freq Control. 1992; 39(2):262–7. [PubMed: 18263145]
86. McGough RJ, Cindric D, Samulski TV. Shape calibration of a conformal ultrasound therapy array. IEEE Trans Ultrason Ferroelectr Freq Control. 2001 Mar; 48(2):494–505. [PubMed: 11370363]
87. McGough RJ, Wang H, Ebbini ES, Cain CA. Mode scanning: heating pattern synthesis with ultrasound phased arrays. Int J Hyperthermia. 1994 May-Jun;10(3):433–42. [PubMed: 7930811]
88. Treeby BE, Jaros J, Rendell AP, Cox BT. Modeling nonlinear ultrasound propagation in heterogeneous media with power law absorption using a k-space pseudospectral method. J Acoust Soc Am. 2012 Jun; 131(6):4324–36. [PubMed: 22712907]
89. Treeby BE, Cox BT. k-Wave: MATLAB toolbox for the simulation and reconstruction of photoacoustic wave fields. Journal of biomedical optics. 2010; 15(2):021314. [PubMed: 20459236]
90. Wu, L.; Amin, V.; Roberts, R.; Ryken, T. An Interactive HIFU Therapy Planning Using Simulation & Visualization. AIP Conference Proceedings; 2007; p. 150-6.
91. Liu HL, McDannold N, Hynynen K. Focal beam distortion and treatment planning in abdominal focused ultrasound surgery. Medical Physics. 2005; 32:1270. [PubMed: 15984679]
92. Hynynen K, Clement G. Clinical applications of focused ultrasound-the brain. International Journal of Hyperthermia. 2007; 23(2):193–202. [PubMed: 17578343]
93. Aubry, J.; Marsac, L.; Pernot, M.; Tanter, M.; Robert, B.; Martin, Y., et al. IEEE Int Ultrasonics Symposium. 2009. MR-guided ultrasonic brain therapy: High frequency approach; p. 321-4.
94. Gelat P, Ter Haar G, Saffari N. Modelling of the acoustic field of a multi-element HIFU array scattered by human ribs. Phys Med Biol. 2011 Sep 7; 56(17):5553–81. [PubMed: 21828903]
95. Pernot M, Aubry J, Tanter M. Prediction of the skull overheating during high intensity focused ultrasound transcranial brain therapy. IEEE Ultrasonics Symposium. 2004; 00(c):1005–8.
96. Marquet F, Pernot M, Aubry J-F, Montaldo G, Marsac L, Tanter M, et al. Non-invasive transcranial ultrasound therapy based on a 3D CT scan: protocol validation and in vitro results. Phys Med Biol. 2009 May; 54(9):2597–613. [PubMed: 19351986]

97. Yamaya C, Inoue H. Heated Temperature Imaging By Absorption Of Ultrasound. Acoustical Imaging. 2009:473–8.

98. Koizumi, T.; Yamamoto, K.; Nagatani, Y.; Soumiya, H.; Saeki, T.; Yaoi, Y., et al. Propagation of ultrasonic longitudinal wave in the cancellous bone covered by the subchondral bone of bovine femur; Ultrasonics Symposium, 2008 IUS 2008 IEEE; 2008; p. 146-9.

99. Nagatani Y, Mizuno K, Saeki T, Matsukawa M, Sakaguchi T, Hosoi H. Numerical and experimental study on the wave attenuation in bone-FDTD simulation of ultrasound propagation in cancellous bone. Ultrasonics. 2008 Nov; 48(6-7):607–12. [PubMed: 18589470]

100. Nakajima, Y.; Tamura, Y.; Matsumoto, Y. Numerical simulation of transskull focused ultrasound. European Conference on Computational Fluid Dynamics; September 5-8 2006; Egmond aan Zee, The Netherlands. 2006.

101. Yamaya C, Inoue H. Behavior of Propagation and Heating Due to Absorption of Ultrasound in Medium. Japanese Journal of Applied Physics. 2006 May; 45(5B):4429–34.

102. Huang J, Holt RG, Cleveland RO, Roy Ra. Experimental validation of a tractable numerical model for focused ultrasound heating in flow-through tissue phantoms. J Acoust Soc Am. 2004; 116(4):2451. [PubMed: 15532675]

103. Auboiroux V, Dumont E, Petrusca L, Viallon M, Salomir R. An MR-compliant phased-array HIFU transducer with augmented steering range, dedicated to abdominal thermotherapy. Phys Med Biol. 2011 Jun; 56(12):3563–82. [PubMed: 21606558]

104. Petrusca L, Salomir R, Brasset L, Chavrier Fc, Cotton Fc, Chapelon JY. Sector-switching sonication strategy for accelerated HIFU treatment of prostate cancer: in vitro experimental validation. IEEE Trans Biomed Eng. 2010 Jan; 57(1):17–23. [PubMed: 19709958]

105. Fennessy F, Tempany C, McDannold N, So M, Hesley G, Gostout B, et al. Uterine leiomyomas: MR imaging-guided focused ultrasound surgery--results of different treatment protocols. Radiology. 2007; 243(3):885–93. [PubMed: 17446521]

106. Moros EG, Straube WL, Klein EE, Yousaf M, Myerson RJ. Simultaneous delivery of electron beam therapy and ultrasound hyperthermia utilizing scanning reflectors: a feasibility study. Int J Radiat Oncol Biol Phys. 1995; 31(4):893–904. [PubMed: 7860403]

107. Moros EG, Novak P, Straube WL, Kolluri P, Yablonskiy DA, Myerson RJ. Thermal contribution of compact bone to intervening tissue-like media exposed to planar ultrasound. Phys Med Biol. 2004 Mar 21; 49(6):869–86. [PubMed: 15104313]

108. Moros EG, Penagaricano J, Novak P, Straube WL, Myerson RJ. Present and future technology for simultaneous superficial thermoradiotherapy of breast cancer. Int J Hyperthermia. 2010; 26(7): 699–709. [PubMed: 20849263]

109. Chen X, Diederich CJ, Wootton JH, Pouliot J, Hsu IC. Optimisation-based thermal treatment planning for catheter-based ultrasound hyperthermia. Int J Hyperthermia. 2010 Feb; 26(1):39–55. [PubMed: 20100052]

110. Wootton JH, Hsu IC, Diederich CJ. Endocervical ultrasound applicator for integrated hyperthermia and HDR brachytherapy in the treatment of locally advanced cervical carcinoma. Med Phys. 2011 Feb; 38(2):598–611. [PubMed: 21452697]

111. Wootton JH, Ross AB, Diederich CJ. Prostate thermal therapy with high intensity transurethral ultrasound: the impact of pelvic bone heating on treatment delivery. Int J Hyperthermia. 2007 Dec; 23(8):609–22. [PubMed: 18097849]

112. Kotte AN, van Leeuwen GM, Lagendijk JJ. Modelling the thermal impact of a discrete vessel tree. Phys Med Biol. 1999 Jan; 44(1):57–74. [PubMed: 10071875]

113. Pennes HH. Analysis of tissue and arterial blood temperatures in the resting human forearm. J App Phys. 1948; 1:93–122.

114. Flyckt VM, Raaymakers BW, Lagendijk JJ. Modelling the impact of blood flow on the temperature distribution in the human eye and the orbit: fixed heat transfer coefficients versus the Pennes bioheat model versus discrete blood vessels. Phys Med Biol. 2006 Oct 7; 51(19):5007–21. [PubMed: 16985284]

115. Neufeld E, Chavannes N, Samaras T, Kuster N. Novel conformal technique to reduce staircasing artifacts at material boundaries for FDTD modeling of the bioheat equation. Phys Med Biol. 2007 Aug 7; 52(15):4371–81. [PubMed: 17634638]

116. Hirata A, Asano T, Fujiwara O. FDTD analysis of body-core temperature elevation in children and adults for whole-body exposure. Phys Med Biol. 2008 Sep 21; 53(18):5223–38. [PubMed: 18728308]

117. Arkin H, Xu LX, Holmes KR. Recent developments in modeling heat transfer in blood perfused tissues. IEEE Trans Biom Eng. 1994; 41:97–107.

118. Jain RK. Temperature distributions in normal and neoplastic tissues during normothermia and hyperthermia. Ann NY Academy Science. 1980; 335:48–66.

119. Crezee J, Lagendijk JJ. Temperature uniformity during hyperthermia: the impact of large vessels. Phys Med Biol. 1992 Jun; 37(6):1321–37. [PubMed: 1626025]

120. Huang HW, Chen ZP, Roemer RB. A counter current vascular network model of heat transfer in tissues. J Biomech Eng. 1996 Feb; 118(1):120–9. [PubMed: 8833083]

121. Mooibroek J, Lagendijk JJ. A fast and simple algorithm for the calculation of convective heat transfer by large vessels in three-dimensional inhomogeneous tissues. IEEE Trans Biomed Eng. 1991 May; 38(5):490–501. [PubMed: 1874532]

122. Weinbaum S, Jiji LM, Lemons DE. Theory and experiment for the effect of vascular microstructure on surface tissue heat transfer-Part I: Anatomical foundation and model conceptualization. J Biomech Eng. 1984 Nov; 106(4):321–30. [PubMed: 6513527]

123. Craciunescu OI, Raaymakers BW, Kotte AN, Das SK, Samulski TV, Lagendijk JJ. Discretizing large traceable vessels and using DE-MRI perfusion maps yields numerical temperature contours that match the MR noninvasive measurements. Med Phys. 2001 Nov; 28(11):2289–96. [PubMed: 11764035]

124. Raaymakers BW, Kotte AN, Lagendijk JJ. How to apply a discrete vessel model in thermal simulations when only incomplete vessel data are available. Phys Med Biol. 2000 Nov; 45(11): 3385–401. [PubMed: 11098912]

125. Van Leeuwen GM, Kotte AN, Raaymakers BW, Lagendijk JJ. Temperature simulations in tissue with a realistic computer generated vessel network. Phys Med Biol. 2000 Apr; 45(4):1035–49. [PubMed: 10795990]

126. Prishvin M, Zaridze R, Bit-Babik G, Faraone A. Improved numerical modelling of heat transfer in human tissue exposed to RF energy. Australas Phys Eng Sci Med. 2010 Dec; 33(4):307–17. [PubMed: 21174187]

127. Craciunescu OI, Das SK, Poulson JM, Samulski TV. Three-dimensional tumor perfusion reconstruction using fractal interpolation functions. IEEE Trans Biomed Eng. 2001 Apr; 48(4): 462–73. [PubMed: 11322534]

128. Song CW. Effect of local hyperthermia on blood flow and microenvironment: A review. Cancer Research (Supplement). 1984; 44:4721–30.

129. Song, CW.; Choi, IB.; Nah, BS.; Sahu, SK.; Osborn, JL. Microvasculature and perfusion in normal tissues and tumors. In: Seegenschmiedt, MH.; Fessenden, P.; Vernon, CC., editors. Thermoradiotherapy and Thermochemotherapy: Volume 1, Biology, Physiology and Physics. Berlin, New York: Springer-Verlag; 1995. p. 139-56.

130. Dudar TE, Jain RK. Differential response of normal and tumor microcirculation to hyperthermia. Cancer Res. 1984 Feb; 44(2):605–12. [PubMed: 6692365]

131. Waterman FM, Tupchong L, Nerlinger RE, Matthews J. Blood flow in human tumors during local hyperthermia. Int J Radiat Oncol Biol Phys. 1991; 20(6):1255–62. [PubMed: 2045300]

132. Crezee J, Mooibroek J, Lagendijk JJ, van Leeuwen GM. The theoretical and experimental evaluation of the heat balance in perfused tissue. Phys Med Biol. 1994 May; 39(5):813–32. [PubMed: 15552087]

133. Hasgall, PA.; Neufeld, E.; Gosselin, MC.; Klingenböck, A.; Kuster, N. IT'IS Database for thermal and electromagnetic parameters of biological tissues. 2012. www.itis.ethz.ch/databasecited July 11th 2012 Version 2.2

134. Bakker JF, Paulides MM, Christ A, Kuster N, van Rhoon GC. Assessment of induced SAR in children exposed to electromagnetic plane waves between 10 MHz and 5.6 GHz. Phys Med Biol. 2010 Jun 7; 55(11):3115–30. [PubMed: 20463374]

135. Cornelis F, Grenier N, Moonen CT, Quesson B. In vivo characterization of tissue thermal properties of the kidney during local hyperthermia induced by MR-guided high-intensity focused ultrasound. NMR Biomed. 2011 Aug; 24(7):799–806. [PubMed: 21834004]

136. Bakker JF, Paulides MM, Neufeld E, Christ A, Kuster N, van Rhoon GC. Children and adults exposed to electromagnetic fields at the ICNIRP reference levels: theoretical assessment of the induced peak temperature increase. Phys Med Biol. 2011 Aug 7; 56(15):4967–89. [PubMed: 21772085]

137. Van der Gaag ML, De Bruijne M, Samaras T, Van der Zee J, Van Rhoon GC. Development of a guideline for the water bolus temperature in superficial hyperthermia. Int J Hyperthermia. 2006 Dec; 22(8):637–56. [PubMed: 17390995]

138. Arunachalam K, Maccarini PF, Schlorff JL, Birkelund Y, Jacobsen S, Stauffer PR. Design of a water coupling bolus with improved flow distribution for multi-element superficial hyperthermia applicators. Int J Hyperthermia. 2009 Nov; 25(7):554–65. [PubMed: 19848618]

139. Arunachalam K, Maccarini P, Craciunescu O, Schlorff J, Stauffer P. Thermal characteristics of thermobrachytherapy surface applicators (TBSA) for treating chestwall recurrence. Phys Med Biol. 2010; 55(7):1949–69. [PubMed: 20224154]

140. Birkelund Y, Jacobsen S, Arunachalam K, Maccarini P, Stauffer PR. Flow patterns and heat convection in a rectangular water bolus for use in superficial hyperthermia. Phys Med Biol. 2009 Jul 7; 54(13):3937–53. [PubMed: 19494426]

141. Kok HP, de Greef M, Borsboom PP, Bel A, Crezee J. Improved power steering with double and triple ring waveguide systems: the impact of the operating frequency. Int J Hyperthermia. 2011; 27(3):224–39. [PubMed: 21501024]

142. Dewey WC. Arrhenius relationships from the molecule and cell to the clinic. Int J Hyperthermia. 2009 Feb; 25(1):3–20. [PubMed: 19219695]

143. Sherar M, Liu FF, Pintilie M, Levin W, Hunt J, Hill R, et al. Relationship between thermal dose and outcome in thermoradiotherapy treatments for superficial recurrences of breast cancer: data from a phase III trial. Int J Radiat Oncol Biol Phys. 1997 Sep 1; 39(2):371–80. [PubMed: 9308941]

144. Jones EL, Samulski TV, Dewhirst MW, Alvarez-Secord A, Berchuck A, Clarke-Pearson D, et al. A pilot Phase II trial of concurrent radiotherapy, chemotherapy, and hyperthermia for locally advanced cervical carcinoma. Cancer. 2003 Jul 15; 98(2):277–82. [PubMed: 12872345]

145. Jones EL, Oleson JR, Prosnitz LR, Samulski TV, Vujaskovic Z, Yu D, et al. Randomized trial of hyperthermia and radiation for superficial tumors. J Clin Oncol. 2005 May 1; 23(13):3079–85. [PubMed: 15860867]

146. Franckena M, Fatehi D, de Bruijne M, Canters RA, van Norden Y, Mens JW, et al. Hyperthermia dose-effect relationship in 420 patients with cervical cancer treated with combined radiotherapy and hyperthermia. Eur J Cancer. 2009 Jul; 45(11):1969–78. [PubMed: 19361982]

147. Lee HK, Antell AG, Perez CA, Straube WL, Ramachandran G, Myerson RJ, et al. Superficial hyperthermia and irradiation for recurrent breast carcinoma of the chest wall: prognostic factors in 196 tumors. Int J Radiat Oncol Biol Phys. 1998 Jan 15; 40(2):365–75. [PubMed: 9457823]

148. Sreenivasa G, Gellermann J, Rau B, Nadobny J, Schlag P, Deuflhard P, et al. Clinical use of the hyperthermia treatment planning system HyperPlan to predict effectiveness and toxicity. Int J Radiat Oncol Biol Phys. 2003 Feb 1; 55(2):407–19. [PubMed: 12527054]

149. Tyreus PD, Diederich CJ. Theoretical model of internally cooled interstitial ultrasound applicators for thermal therapy. Phys Med Biol. 2002 Apr 7; 47(7):1073–89. [PubMed: 11996056]

150. Das SK, Clegg ST, Anscher MS, Samulski TV. Simulation of electromagnetically induced hyperthermia: a finite element gridding method. Int J Hyperthermia. 1995 Nov-Dec;11(6):797–808. [PubMed: 8586901]

151. Stalling, D.; Seebass, M.; Hege, H.; Wust, P.; Deuflhard, P.; Felix, R. Papers, Proc 7th Int Congress on Hyperthermic Oncology. In: Franconi, CGA.; Cavaliere, R., editors. Hyperthermic Oncology. Rome: Tor Vergata; 1996. p. 552-4.

152. Gellermann J, Goke J, Figiel R, Weihrauch M, Cho CH, Budach V, et al. Simulation of different applicator positions for treatment of a presacral tumour. Int J Hyperthermia. 2007 Feb; 23(1):37–47. [PubMed: 17575722]

153. Canters RA, Franckena M, van der Zee J, Van Rhoon GC. Complaint-adaptive power density optimization as a tool for HTP-guided steering in deep hyperthermia treatment of pelvic tumors. Phys Med Biol. 2008 Dec 7; 53(23):6799–820. [PubMed: 19001699]

154. Yuan Y, Cheng KS, Craciunescu OI, Stauffer PR, Maccarini PF, Arunachalam K, et al. Utility of treatment planning for thermochemotherapy treatment of nonmuscle invasive bladder carcinoma. Med Phys. 2012 Mar; 39(3):1170–81. [PubMed: 22380348]

155. Li Z, Maccarini PF, Arabe OA, Stakhursky V, Joines WT, Stauffer PR, et al. Towards the validation of a commercial hyperthermia treatment planning system. Microwave J. 2008 Dec; 51(12):28–42.

156. Stakhursky VL, Arabe O, Cheng KS, Macfall J, Maccarini P, Craciunescu O, et al. Real-time MRI-guided hyperthermia treatment using a fast adaptive algorithm. Phys Med Biol. 2009 Mar 13; 54(7):2131–45. [PubMed: 19287081]

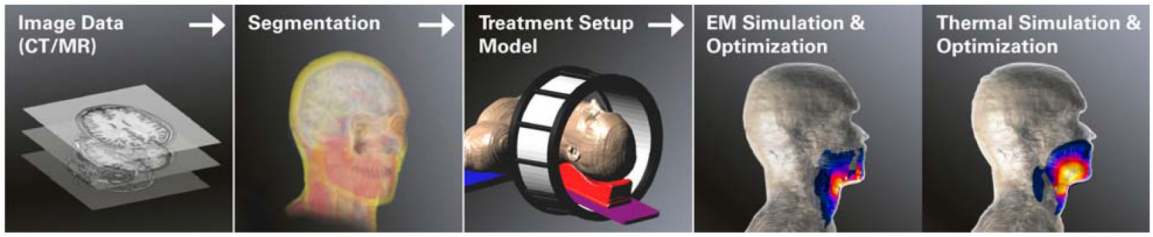

Figure 1.
Schematic workflow for EM-HTP, using head and neck hyperthermia as example. In US-HTP the EM simulation & optimization step is replaced by US simulation & optimization.

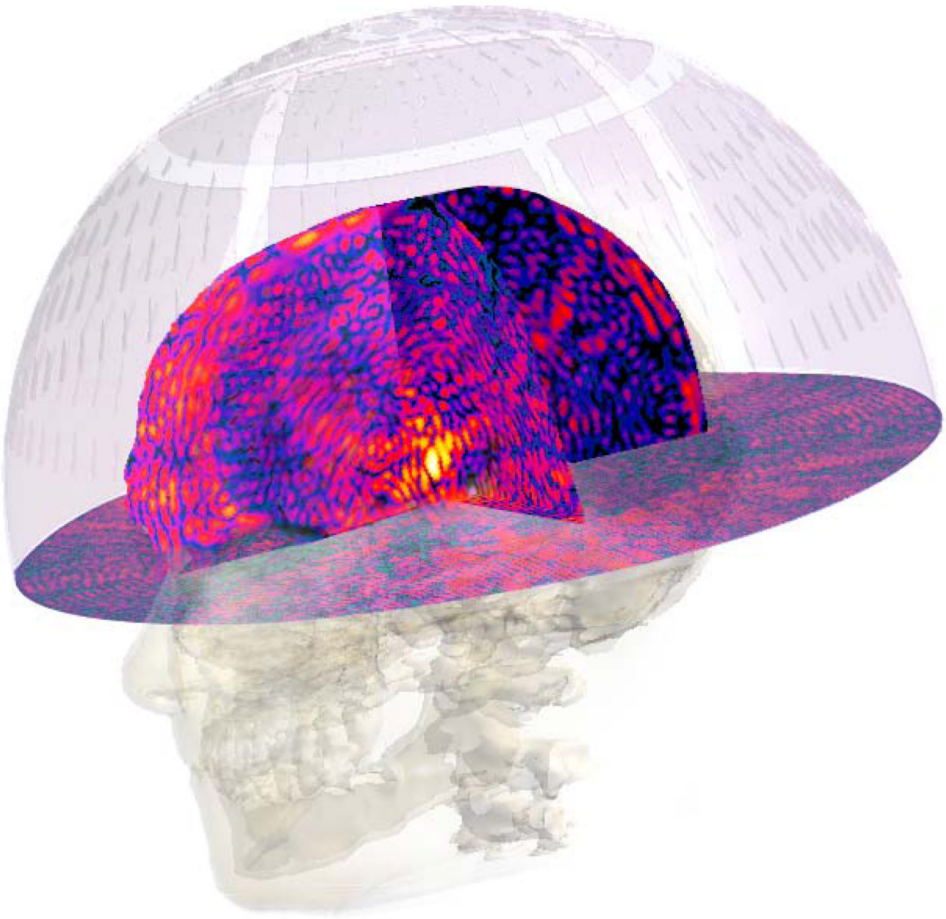

Figure 2.
US pressure field prediction for a model of the InSightec ExAblate4000 system, illustrating the feasibility of 3D full-wave simulation for this system with 1024 independently driven transducers. The obtained pressure distribution is displayed with a logarithmic color scale on three orthogonal planes through the target. The distorting impact of tissue parameter inhomogeneity on the focus shape is clearly visible. Modeling allows to plan dynamic focus scanning, for contiguous heating of large tissue volumes.

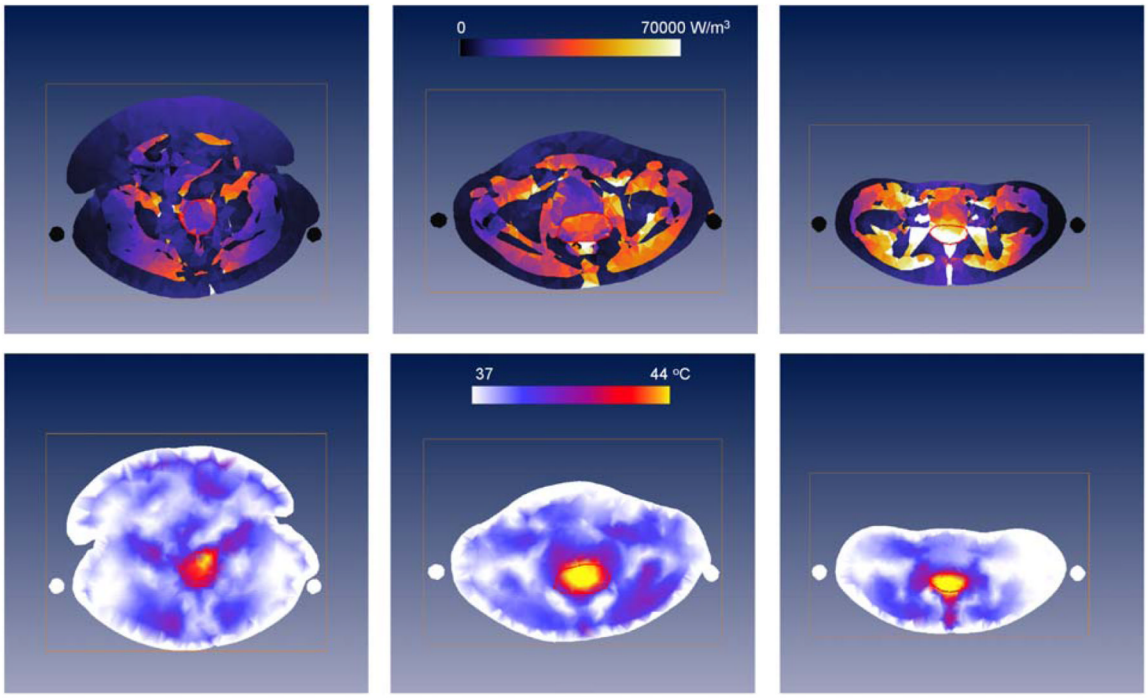

Figure 3.
Cross-sections of the PD for 400W (upper row) and temperature distributions (lower row) predicted by Sigma-HyperPlan for a large (left), average (middle) and slim (right) patient with a cervical tumor (red contour). Visible are also the slings on which the patient is positioned during deep HT (black or white circles on each side of the patient). The temperature distributions are obtained by increasing power until 44°C in healthy tissue is reached.

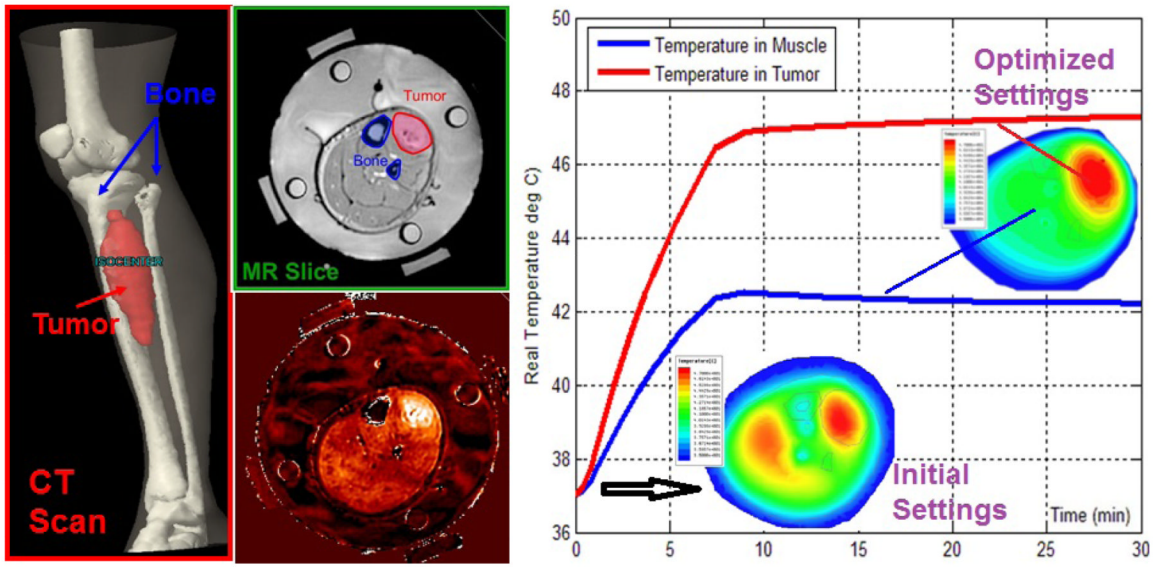

Figure 4.

Combined use of segmentation, EM, and thermal solvers to generate initial temperature distributions in the pretreatment phase. During treatment, the MR temperature imaging (MRTI) provides feedback to empirically determine patient specific parameters, e.g., perfusion. This information was used to steer the beam effectively to the target tumor on right side of leg and away from muscle at the left of bone (67, 155).